# Synthesis, Characterization and Adsorption Studies of a Graphene Oxide/Polyacrylic Acid Nanocomposite Hydrogel

**Makarim A. Mahdi[1], Aseel M. Aljeboree[2], Layth S. Jasim[3], Ayad F. Alkaim[4*]**

## Abstract

The AAc/GO nanocomposite hydrogel was successfully employed as a polymeric Nano sorbent of the removal efficiency of M G dye from the model. The complication of the mechanism of the adsorption system was completely exposed by examining how solution pH affects adsorption, Ionic strength isotherm models, kinetic models, and thermodynamics. The adsorption of the MG dye was greatly dependent on the solution pH. The Freundlich model has been demonstrated to be the most accurate in describing the MG dye sorption, whilst the Langmuir model was shown to be the least accurate. Additionally, these integrated mechanisms fit nicely within the framework of a pseudo-second-order model. Additionally, the contact time at equilibrium short (ten minutes) required to MG removes demonstrates the AAc/GO nanocomposite hydrogel can be considered an efficient and potentially useful adsorbent for MG removal from industrial effluents.



**Key Words:** Adsorption, Dye, Isotherm, Hydrogel, Kinetic, Thermodynamic.

**DOI Number: 10.14704/nq.2021.19.9.NQ21136** **NeuroQuantology 2021; 19(9):46-54**

## Introduction

Water contamination has been one of the most critical global concerns since it poses a severe environmental danger, threatens human health, (J.R.C. Rocha, 2002), and disrupts symbiotic processes in aquatic bio-systems, resulting in decreased photosynthetic activity (El-Mossalamy, 2004). Contamination of water can occur as a result of the discharge of poisonous colors, additives, organic contaminants, and toxic heavy metal ions (Shama, 2002). Wastewater from a variety of industries, counting metallurgical manufacture, mining, and others, contains the same dangerous metal ions (Riegel and Ellis, 1994). Dyes are colorful organic compounds with chromophoric ($NR_2$, NHR, $NH_2$, COOH, and OH) and auxochrome ($N_2$, NO, and $NO_2$) functional groups (Speltini et al). As a result, successful ways for removing dyes from water have been investigated, as well as new publications in the literature. As a result, a variety of strategies have been investigated for the removal of organic pollutants from waste water, counting biological approaches and chemical oxidation (Ruwaida A Raheem, 2016), coagulation (J.M. Nugent, 2001, F. Valentini, 2003), photocatalytic process (Ayad F. Alkaim 2016, Guo et al., 2004, Ayad F Alkaim, 2016) membrane separation (Y. Zhao, 2002) and adsorption processes (ALYAA KAREEM, 2016, Barisci* et al., 2000).

**Corresponding author:** Ayad F. Alkaim

**Address:** [1]Department of Chemistry, College of Education, University of Al-Qadisiyah, Diwaniya, Iraq; [2]Department of Chemistry, College of Sciences for Girls, University of Babylon, Hilla, Iraq; [3]Department of Chemistry, College of Education, University of Al-Qadisiyah, Diwaniya, Iraq; [4*]Department of Chemistry, College of Sciences for Girls, University of Babylon, Hilla, Iraq.

[4*]E-mail: alkaimayad@gmail.com

**Relevant conflicts of interest/financial disclosures:** The authors declare that the research was conducted in the absence of any commercial or financial relationships that could be construed as a potential conflict of interest.

**Received:** 03 July 2021 **Accepted:** 10 August 2021

Among these approaches, adsorption has garnered considerable attention because to its better effectiveness, recyclability of the sorbent, simplicity, and applicability to a wide variety of dyes (Wang et al., 2007, Ware, 1992).

A variety of adsorbents have been produced and characterized. It should be noted that some adsorbents have drawbacks such as decreased efficiency, sludge formation, and increased costs. As a result, there is a need to design some simple adsorbents with a low-cost preparation process and increased efficiency. In this study, we demonstrate the efficacy of dye removal using a highly high-efficiency surface nanocomposite hydrogel that is both affordable and environmentally safe.

## Materials and Methods

### *Chemicals*

Acrylic acid (AA), potassium persulphate, and acetic acid are obtained from Sigma-Aldrich, Sodium hydroxide, (NaOH), hydrochloric acid, (HCl), and Sodium nitrate ($NaNO_3$) were both obtained from Merck, Malaysia.

### *Preparation of Acrylic Acid / Graphene Oxide (AAc / GO) Composite*

Prepared graphene oxide by a modified Hummer method to surly converted all graphite to graphene oxide. We added 30% hydrogen peroxide, then 10% HCl and barium chloride put it in a furnace at 40°C for a whole day. Dispersing one gram from Graphene oxide in one liter of DI water. Before usage, the dispersion (0.001g. $mL^{-1}$) was subjected to 12 hours of ultrasonic oscillations. A predetermined concentration of acrylic acid was introduced to a three-necked flask equipped with a condenser, a thermometer, and a nitrogen line. The flask was filled with a predetermined amount of graphene oxide dispersion. After 40 minutes of vigorous agitation, the mixture was putted in a water bath at 50°C. The MBA solution (0.003 g. $mL^{-1}$) was then added to the flask while maintaining a nitrogen atmosphere in the flask. The water bath was gradually warmed to 65°C after 40 minutes of stirring at 50°C. KPS solution was added to the flask (0.03 g. $mL^{-1}$). After approximately two hours of reaction, a black gel AAc/GO nanocomposite hydrogel was formed. After bringing the hydrogels to room temperature, they were repeatedly rinsed in deionized water, cut into little pieces, dried, and then ground for future use.

### *Adsorption Experiments*

A one thousand mg $L^{-1}$ standard solution has been made through dissolution of one gram of MGdye in one thousand milliliter of D.W. Dilutions of stock solutions in an adequate volume of DW were used to prepare the required experimental concentrations. Dye solutions (10 mL) were placed inside locked conical flask consist of 0.05 g of AAc/GO nanocomposite hydrogel at specified concentrations (10–100 mg/L). Adsorption studies on prepared MG solution were conducted in a water bath shaker at a temp. of 25°C and a speed of 240 r/m. Different adsorption tests was performe in order for improve expermental parameters like the solution's starting pH and temperature. The pH values (3.0–10.0) were set to the measuring MG dye initial concntration of 100 mg $L^{-1}$. The pH of MG solution was regulated utilizing 0.1 M Sodium hydroxide and 0.1 M Hydrochloric acid. In each exemplary batch experiment, 0.05g of the AAc/GO nano composite hydrogel was immersed in10 mLof solution dye with an primary conc. of 100 mg $l^{-1}$. At certain times, samples were withdrawn from the water bath and the suspensions were filtered. The percent of dye adsorption measured using a UV-VIS spectrophotometer match to a wavelength of 590 nanometer (Shimadzu, UV-2450, UV-Vis spectrophotometer). The elimination percentage (E%) and adsorption efficiency were calculated using the following formulae (qe).(Aljeboree et al., 2019):

$$Qe = \frac{Co - Ce}{W} * V \quad (1)$$

$$E\% = \frac{Co - Ce}{Co} * 100 \quad (2)$$

$C_o$ (mg. $L^{-1}$) the primary conc. of MV, and $C_e$ (mg. $L^{-1}$) is the dye equilibrium concentration at time t (min), W (g) mass of adsorbent, V (L) is the volume of MV solution.

## Results and Discussion

### *Characterization of the Adsorbent*

The FTIR data of the surface AAc/GO before and AAc/GO-MG after adsorption is exposed in Figure (1). The results show no significant change among the surface before, after adsorption. For each prominent peak, it might be proposed that it represents the dominant peak of AAc/GO before adsorption. The spectra exhibited the fundamental vibration modes–OH (3490$cm^{-1}$), and C=O (1626$cm^{-1}$) (Yiming Li 2017). In addition, the bands

around 1458cm$^{-1}$ resulted from $CO_2$ adsorption during sample fabrication. The major FTIR band assignments for the surface before and after adsorption in the 4000–400cm$^{-1}$ region are presented in Figure (1). As a result, AAc/GO-MG retained a comparable structure to AAc/GO upon adsorption. Additionally, We note that the intensity of the band for a surface after adsorption is higher than the intensity of the band before adsorption as a result of merging the dye with the surface (Nadher D. Radhy, 2019, Hoppen et al., 2019).

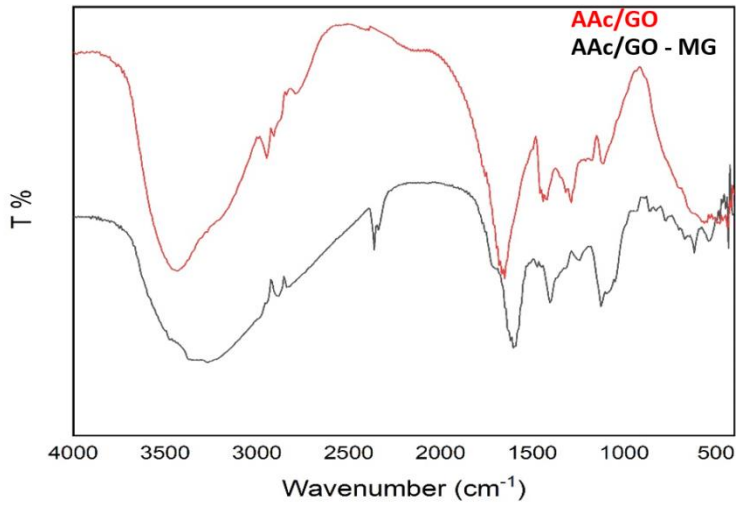


**Fig. 1.** FT-IR spectra of AAc/GO nanocomposite hydrogel surface before, and after adsorption of MG dye

Through Figure (2), it is clear that the surface nanocomposite AAc/GO nanocomposite hydrogel before adsorption was smooth and cloud-like, without potholes (Chen et al., 2019). But after loading the MG dye, the surface became containing many cavities and sphere-like particles, irregular, this is an indication of the dye's interference with the surface nanocomposite hydrogel (Arya and Philip, 2016, Layth S. Jasim, 2021).



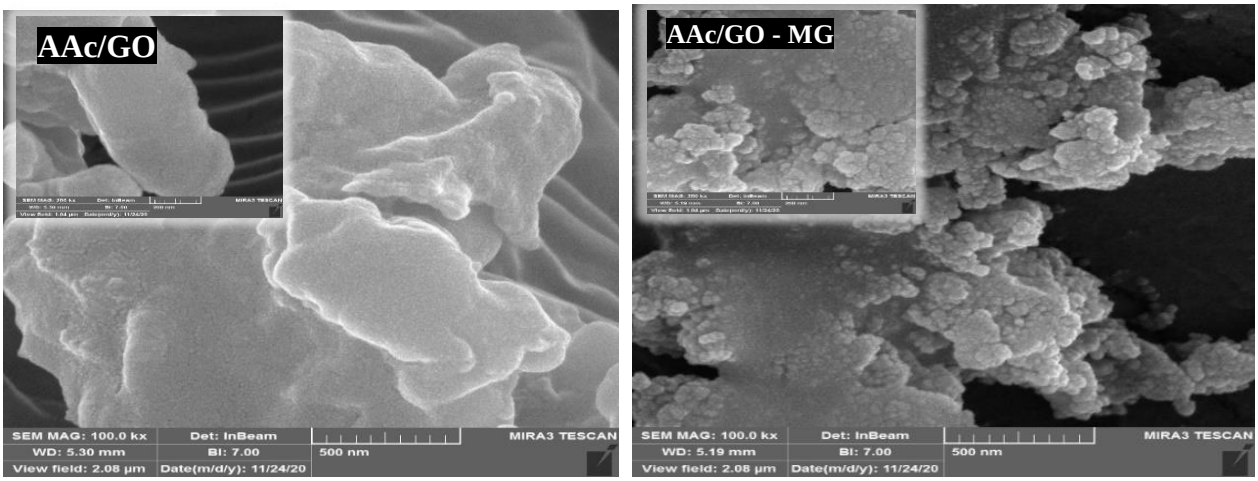


**Fig. 2.** FESEM image of AAc/GO nanocomposite hydrogel before and after adsorption of MG dye

The curve of the TGA for the AAc/GO nanocomposite hydrogel Figure (3) appear two stages of a gradual decrease in mass by rise in temp from 50 to 900°C. The first stage occurs at (60-133.5)°C because loss of water molecules or moisture (Abbas N. Karim, 2019). The second stage occurs at (133.5-267.8)°C, because of decar-boxylation and estimation of the nanocomposite chain as a gas CO2 and NH3, at the same order. The third stage occurs at (267.80-444)°C The fourth stage occurs at (344-550)°C, because of degradation of the AAc/GO Nano composite hydrogel chain(Shen et al., 2018).

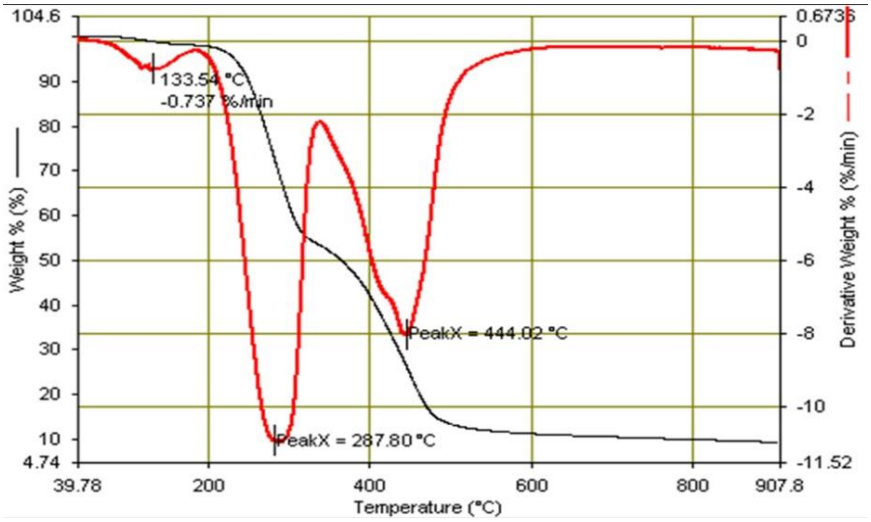


**Fig. 3.** TGA of the AAc/GO nanocomposite hydrogel

The X.R.D of the AAc/GO nanocomposite Figure (4) appear a main broad peak at position (2θ = 22.124 °) and d-spacing of (d = 4.397A°); this refers to the noncrystalline nature of AAc/GO (Dai et al., 2017, French, 2014).

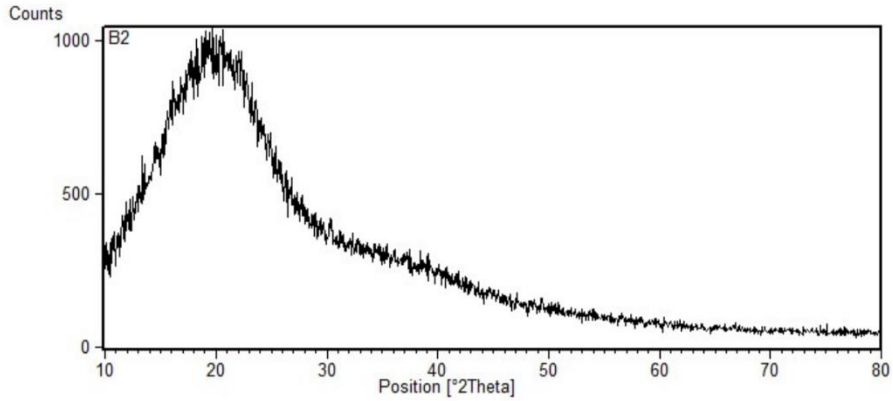


**Fig. 4.** XRD of the AAc/GO nanocomposite hydrogel



## *Solution pH Effect*

Removal Percentage (%E) for pollutant MG dye, the capacity of adsorption ($q_e$ mg/g) have been determined and shown in Figure (5). presents the influence of solution pH on the percentage removal of MG utilizing AAc/GO nanocomposite hydrogel. The selected MG dye illustrates different adsorption behavior. when increases solution of pH the percentage removal of MG dye decrease, pH 6 to 10 will decrease in rapidity, increasing the pH of the solution and removal percentage and adsorption capacity of MG dye increases were as follows: from (94.82%) to (98.85%) and (18.9 mg/g) to (19,6mg/g) at the same order for an increase in pH from 3.2 to 10.5. This observation can be explained in the case of MG dye adsorption by an ion exchange and electrostatic repulsion or attraction among the formed adsorbent and the adsorbate (dye) that occurs during the adsorption method. (Layth S. Jasim 2018, Jasim M. Salman, 2016). Therefore, this adsorption method also results in a low or high elimination % of the MG dye impurity. Additionally, the charge on the surface of the nanocomposite hydrogel must be addressed when examining the effect of solution pH. This finding further establishes that the charge on the adsorbent surface does not affect dye adsorption. Thus, the optimal pH solution for maximal dye adsorption was determined to be pH 3. The remainder of the investigation was conducted using these optimal pH settings. (Muhammad Nadeem Zafar, 2019).

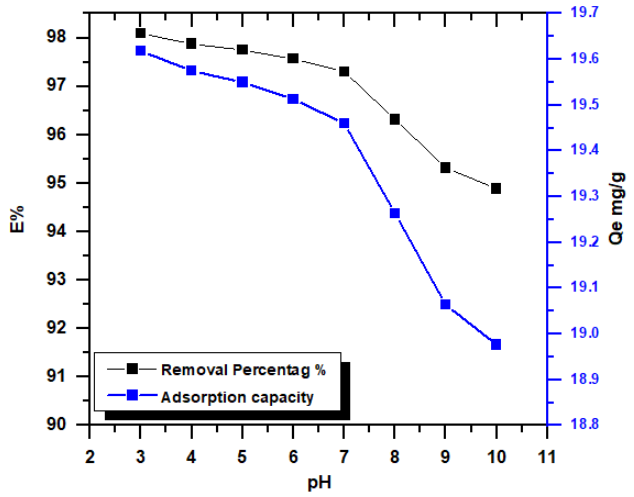


**Fig. 5.** Effect of pH solution on the percent removal and adsorption capacity onto AAc/GO nanocomposite hydrogel (Exp. Condition: Temp. = 25°C, contact time 1 hr., amount of adsorbent 0.05 gm)

## *Effect of Ionic Strength*

The results in Figure (6) indicate that the amount of adsorbate on the surface increases when the concentration of sodium or potassium chloride increases, while calcium carbonite has a negligible influence on adsorption. incorporated into the solution. This is because the dye's solubility in the solution decreases due to the interaction of the salt ions and the solvent molecules. Salt ions and dye ions compete for interaction with the solvent. The calcium carbonate, the positive charge on the calcium Ca+2 composes a complex with the negative part of the MG dye, which makes the adsorption less likely (Abbas N. Karim, 2019).

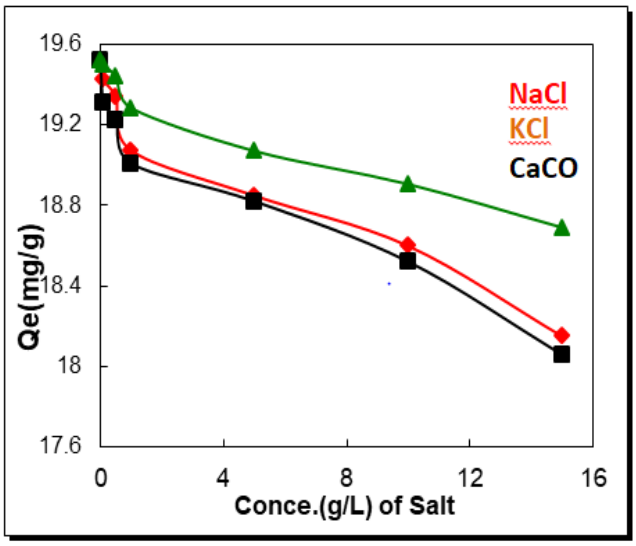


**Fig. 6.** The salt effects adsorption of dye (MG) on surface AAc/GO nanocomposite hydrogel

## *Adsorption Thermodynamics*

The effect was investigated at different solution temperatures where, 10, 20,25, 60, and 30 °C were taken into consideration to demonstrate the effect of temperature on MG dye solution using pH 6.8, 225 r/m, and 0.05 g of adsorbent for 2 h to achieve equilibrium. At the end of 2 h, the samples were filtered and the residual conc. of MG in the filtrate were analyzed by a UV–V Spectrophotometer. The highest removal percentage E% was stated to be at 30°C which represents 98.83 % and the lowest removal percentage E% was at 10°C which represents 93.33 %. results are presented in Figure (7). The factors of thermodynamic were estimation utilizing the Van't Hoff equation (3).

$$\Delta G° = -RT \ln K \quad (3)$$

According to law thermo-dynamic law, the Van't Hoff equation (Eq. (4)) estimation by

$$\Delta G° = \Delta H° - T\Delta°S \quad (4)$$

Eq. (5) above can be further transformed as follows [3]:

$$\ln k = - \Delta G°/RT = - \Delta H°/RT + \Delta S°/R \quad (5)$$

where T is the temp. solution (K), Ka is the adsorption equilibrium constant, and R is the gas constant. ($\Delta H^o$) and ($\Delta S^o$) were calculated from the slope and intercept from the plot of ln ($X_m$) versus 1000 K/T (Figure (8). Organic compound adsorption is an exothermic process, and the physical interaction between the organic compounds and the active sites of AAc/GO nanocomposite hydrogel and related adsorbents weakens as the temperature increases (Waleed K. Abdulsahib, 2020). When dye adsorption is exothermic, increasing the temp increases the MV adsorption rate but decreases the total adsorption capacity (M. Chiban, 2016). If diffusion is the rate-limiting phase, increasing the temperature results in an increase in the dye molecule's diffusivity and, subsequently, in the absorption rate. Additionally, the temperature affects the reversibility of the adsorption equilibrium and the desorption step (Table 1).

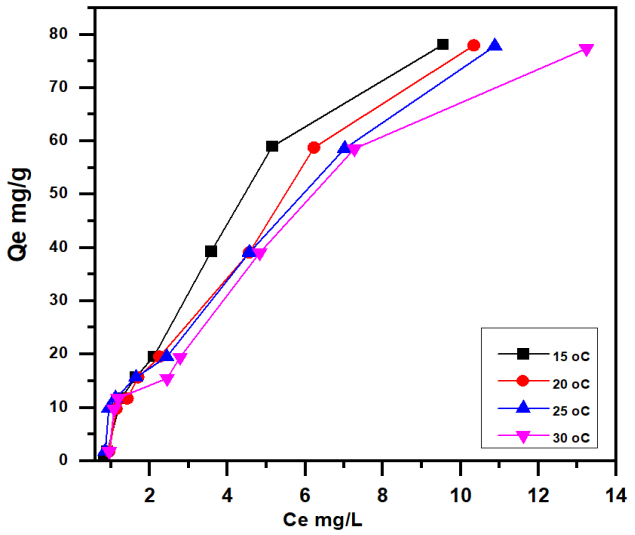


**Fig. 7.** Adsorption isotherms of MG dye on AAc/GO nanocomposite hydrogel at different temperatures

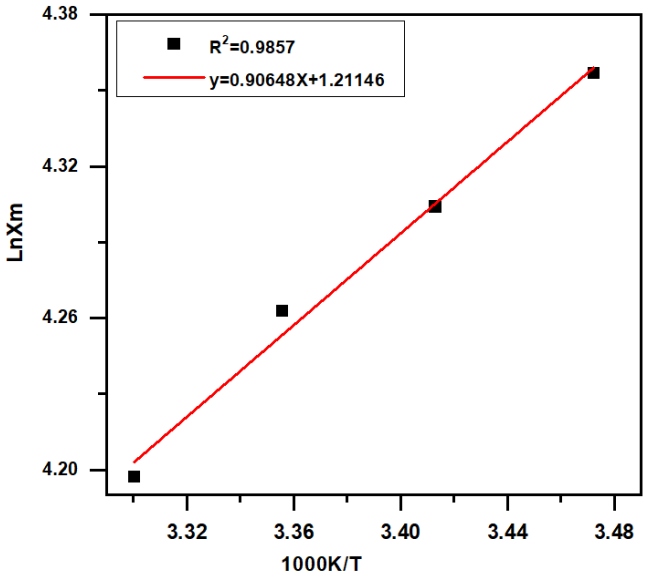


**Fig. 8.** Plot ln $X_m$ against the absolute temp. of the adsorption (MG) on to AAc/GO hydrogel

**Table 1.** Thermodynamic factors for MG dye adsorption on AAc/GO hydrogel

| ΔH (KJ.mol$^{-1}$) | ΔG (kJ.mol$^{-1}$) | Equilibrium constant | ΔS (J.mol$^{-1}$. K$^{-1}$) |
|---|---|---|---|
| -7.536 | -5.023 | 46752.350 | 10.072 |
| | -4.982 | 38662.480 | |
| | -4.965 | 37095.080 | |
| | -4.883 | 34743.990 | |

## *Adsorption Isotherms*

The experimental result for the percentage removal of MG dye were tested with several models Langmuir, Freundlich isotherm. sorption models are applied to study the isotherm for adsorption of MG dye on the hydrogel. The mathematical forms of the two models Freundlch, Langmuir are expressed by eq. (6 and 7), respectively.

The Freundlch isotherm model is commonly applied to the hetero-geneous solid catalyst and is a mathematical relation utilized to describe multi-layer adsorption. Langmuir model states that during the adsorption method the mono-layer is formed when there is no interaction among adsorbate molecules(M. Chiban, 2016).

$$Qe = \frac{Qm\ KL\ Ce}{1+KL\ Ce} \qquad (6)$$

$$Qe = K_f Ce^{1/n} \qquad (7)$$

While $K_f$ (L/mg) is constant Freundlch, 1/n is the hetero-geneity parameter. These two isotherm equation constants along with the $R^2$ values are calculated as shown in Table 2 and the correlated adsorption isotherm are shown in Figure (9). From Table 2, the correlation coefficient, $R^2$ values for the Langmuir, Freundlich model at different temperate (10,20, 25 and 30°C) are (0.90413, 0.9765, 0.91703 and 0.9393) respectively.

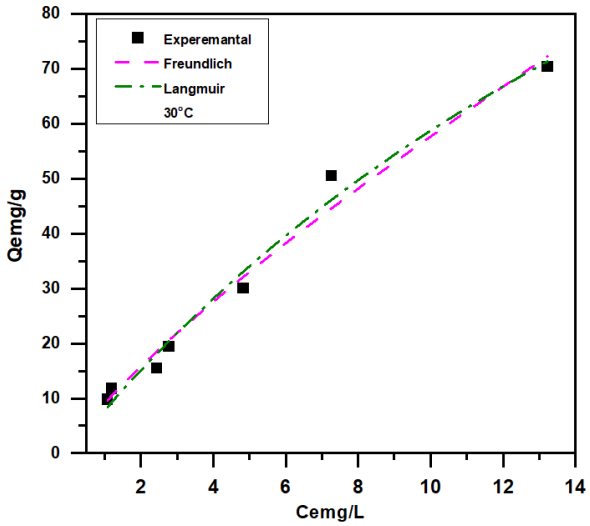


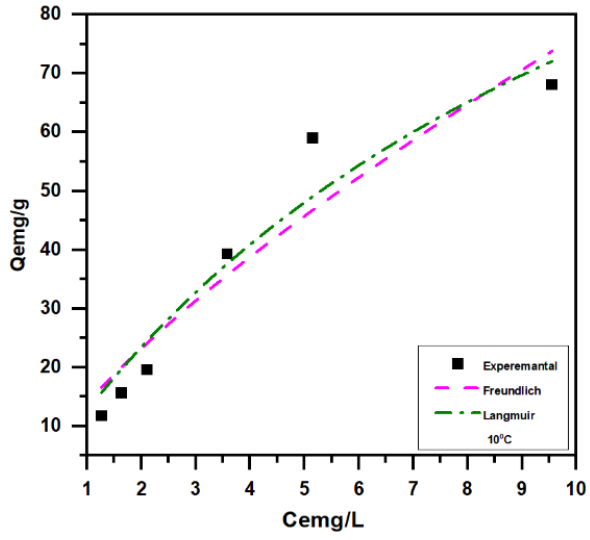

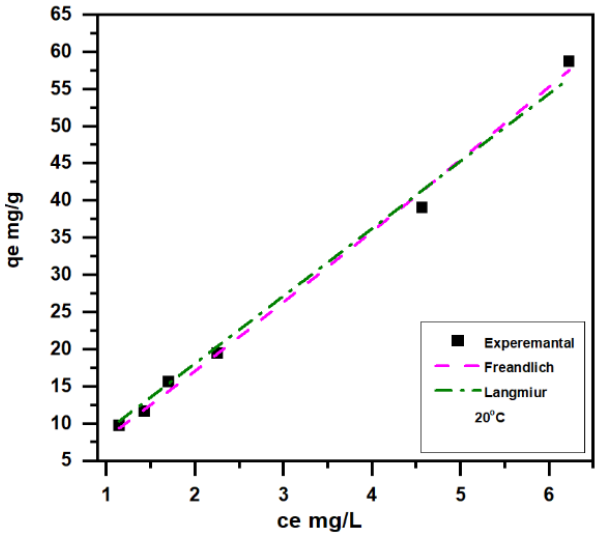


**Fig. 9.** Several adsorption models nonlinear fit of adsorption MG dye onto AAc/GO nanocomposite hydrogel. at different temperatures conc.

**Table 2.** Different factors models for the adsorption study of MG dye on to AAc/GO nanocomposite hydrogel at different temperatures

| AAc/GO nanocomposite hydrogel | | | | |
|---|---|---|---|---|
| **Temperature/ °C** | | **10°C** | **20°C** | **30°C** |
| **Freundlich** | $K_F$ | 13.897 ± 3.575 | 8.1579 ± 0.582 | 9.031 ± 1.177 |
| | 1/n | 0.740 ± 0.134 | 1.0681 ± 0.044 | 0.8019 ± 0.057 |
| | $R^2$ | 0.9249 | 0.9944 | 0.9789 |
| **Langmuir** | $q_m$ (mg.g-1) | 159.962 ± 59.871 | 656.08 ± 7.1823 | 118.246 ± 11.383 |
| | $K_L$(L.mg-1) | 0.085 ± 0.004 | 1.382 ± 0.0151 | 0.005 ±0.906 |
| | $R^2$ | 0.8867 | 0.9910 | 0.9396 |

## Adsorption Kinetics

### *Lagergren First Order Equation*

The following first-order rate formula is utilized to determine the adsorption rate constant. (Lagergren, 1898):

$$\ln(q_e-q_t) = \ln q_e - k_1 t \qquad (6)$$

The quantity of MV adsorbed at equilibrium, qe, is equal to the amount of dye adsorbed over time, qt, divided by the rate constant of adsorption, k1. The rate constant, k1, was estimation via using the linear plot of the graph and found in Table 3.

### *Second Order Kinetics Equation*

The adsorption method kinetics can alternatively be characterized using a second-order rate equation (Ho, 1998). The linearized version of t is as follows:

$$\frac{1}{qt} = \frac{1}{K2qe2} + \frac{1}{qe}\, t \qquad (7)$$

Table 1 summarizes the kinetic parameters for dye adsorption on the AAc/GO nanocomposite hydrogel surface (3). Where it is noted that the adsorption process is very applicable to second models with correlation coefficients up to $R^2$ = 0.9834. While applicability to the pseudo-first-order model diminishes as the correlation coefficient drops up to $R^2$ = 0.9479 (Ghaedi, 2012, Acero, 2010., Kalithasan Natarajan, 2016).

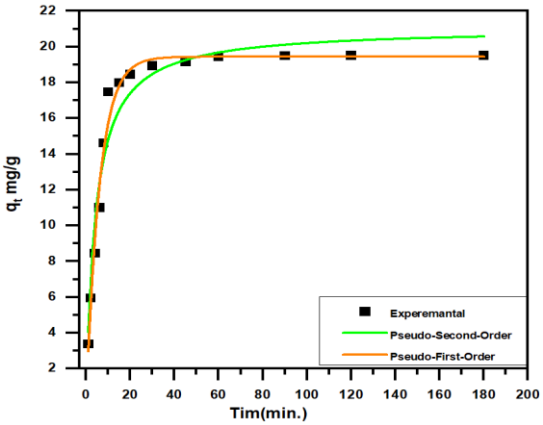


**Fig. 10.** Adsorption rate curves MG dye: experimental conditions: pH 6, dye conc. 100 mg/L, Temp. 298 K and mass catalyst 0.05 g).



**Table 3.** Adsorption kinetics factors the adsorption of MG dye

| Model | Equation | Parameters | Value |
|---|---|---|---|
| **First-order** | $q_t=q_e[1-\exp(k_f t)]$ | K1(min-1) | 0.234 ± 0.0346 |
| | | qe(calc.) (mg.g-1) | 21.055 ± 0.6406 |
| | | R2 | 0.9479 |
| **Second-order** | $q_t=\frac{K2qe2t}{1+K2qet}$ | K2(g/mg.min-1) | 0.1661 ± 0.0095 |
| | | qe(calc.) (mg.g-1) | 19.442 ± 0.2809 |
| | | h(mg.g-1.min) | 6.2781 |
| | | $R^2$ | 0.9834 |

## Conclusion

It was confirmed through the experiments used in this study that the prepared nanocomposite AAc/GO nanocomposite hydrogel surface has very high efficiency in removing pollutants. In terms of adsorption, the rate-controlling step was described using a kinetic second model (qt = 19.45 mg.g-1 at pH 6.0), and the adsorption model were fitted using the model Freundlich ($q_e$ = 70.400 mg.g-1 at pH 6.0), which accounted for approximately 94 percent of the MG dye adsorption efficiency on to AAc/GO nanocomposite hydrogel. The thermodynamic

results indicated that the MG dye was adsorbing via exothermic mechanisms.

## References

Karim AN, Jasim LS. Synthesis and Characterization of Poly (CH/AA-co-AM) Composite: Adsorption and Thermodynamic Studies of Benzocaine on from Aqueous Solutions. *International Journal of Drug Delivery Technology* 2019; 9(4): 558-562.

Acero JL, Benitez FJ, Real FJ, Roldan G. Kinetics of aqueous chlorination of some pharmaceuticals and their elimination from water matrices. *Water Research* 2010; 44(14): 4158-4170.

Aljeboree AM, Alshirifi AN, Alkaim AF. Activated carbon (as a waste plant sources)–clay micro/nanocomposite as effective adsorbent: process optimization for ultrasound-assisted adsorption removal of amoxicillin drug. *Plant Archives* 2019; 19(2): 915-919.

Kareem A, Abd Alrazak N, Aljebori KH, Aljebori AM, Algboory HL, Alkaim AF. Removal of methylene blue dye from aqueous solutions by using activated carbon/ urea-formaldehyde composite resin as an adsorbent. *International Journal of Chemical Sciences* 2016; 14(2): 635-648.

Arya V, Philip L. Adsorption of pharmaceuticals in water using Fe3O4 coated polymer clay composite. *Microporous and Mesoporous Materials* 2016; 232: 273-280.

Alkaim AF, Kandiel TA, Dillert R, Bahnemann DW. Photocatalytic hydrogen production from biomass-derived compounds: a case study of citric acid. *Environmental technology* 2016; 37(21): 2687-2693.

Alkaim AF, Alrobayi EM, Algubili AM, Aljeboree AM. Synthesis, characterization, and photocatalytic activity of sonochemical/hydration–dehydration prepared ZnO rod-like architecture nano/microstructures assisted by a biotemplate. *Environmental technology* 2017; 38(17): 2119-2129.

Alkaim AF, Alrobayi EM, Algubili AM, Aljeboree AM. Synthesis, characterization, and photocatalytic activity of sonochemical/hydration–dehydration prepared ZnO rod-like architecture nano/microstructures assisted by a biotemplate. *Environmental technology* 2017; 38(17): 2119-2129. http://doi.org/10.1080/09593330.2016.1246615

Barisci JN, Wallace GG, Baughman RH. Electrochemical studies of single-wall carbon nanotubes in aqueous solutions. *Journal of Electroanalytical Chemistry* 2000; 488(2): 92-98.

Chen Q, Zhu R, Fu H, Ma L, Zhu J, He H, Deng Y. From natural clay minerals to porous silicon nanoparticles. *Microporous and Mesoporous Materials* 2018; 260: 76-83.

Dai H, Ou S, Liu Z, Huang H. Pineapple peel carboxymethyl cellulose/polyvinyl alcohol/mesoporous silica SBA-15 hydrogel composites for papain immobilization. *Carbohydrate polymers* 2017; 169: 504-514.

El-Mossalamy EH. Charge-transfer complexes of phenylephrine with nitrobenzene derivatives. *Spectrochimica Acta Part A: Molecular and Biomolecular Spectroscopy* 2004; 60(5): 1161-1167.

Valentini F, Amine A, Orlanducci S, Terranova ML, Palleschi G. Carbon nanotube purification: preparation and characterization of carbon nanotube paste electrodes. *Analytical chemistry* 2003; 75(20): 5413-5421.

French AD. Idealized powder diffraction patterns for cellulose polymorphs. *Cellulose* 2014; 21(2): 885-896.

Ghaedi M, Sadeghian B, Pebdani AA, Sahraei R, Daneshfar A, Duran CELAL. Kinetics, thermodynamics and equilibrium evaluation of direct yellow 12 removal by adsorption onto silver nanoparticles loaded activated carbon. *Chemical Engineering Journal* 2012; 187: 133-141.

Guo M, Chen J, Nie L, Yao S. Electrostatic assembly of calf thymus DNA on multi-walled carbon nanotube modified gold electrode and its interaction with chlorpromazine hydrochloride. *Electrochimica Acta* 2004; 49(16): 2637-2643.

Ho YS, McKay G. Sorption of dye from aqueous solution by peat. *Chemical engineering journal* 1998; 70(2): 115-124.

Hoppen MI, Carvalho KQ, Ferreira RC, Passig FH, Pereira IC, Rizzo-Domingues RCP, Bottini RCR. Adsorption and desorption of acetylsalicylic acid onto activated carbon of babassu coconut mesocarp. *Journal of Environmental Chemical Engineering* 2019; 7(1): 102862.

Nugent JM, Santhanam KSV, Rubio AA, Ajayan PM. Fast electron transfer kinetics on multiwalled carbon nanotube microbundle electrodes. *Nano letters* 2001; 1(2): 87-91.

Rocha JR, Galhardo CX, Natividade MAE, Masini JC. Spectrophotometric determination of phenylephrine hydrochloride in pharmaceuticals by flow injection analysis exploiting the reaction with potassium ferricyanide and 4-aminoantipyrine. *Journal of AOAC International* 2002; 85(4): 875-878.

Salman JM, Abdul-Adel E, AlKaim AF. Effect of pesticide Glyphosate on some biochemical features in cyanophyta algae Oscillatoria limnetica. *International Journal of PharmTech Research* 2016; 9(8): 355-365.

Natarajan K, Bajaj HC, Tayade RJ. Photocatalytic efficiency of bismuth oxyhalide (Br, Cl and I) nanoplates for RhB dye degradation under LED irradiation. *Journal of industrial and engineering chemistry* 2016; 34: 146-156.

Lagergren SK. About the theory of so-called adsorption of soluble substances. *Sven. Vetenskapsakad. Handingarl* 1898; 24: 1-39.

Layth S, Jasim AMA. Removal of Heavy Metals by Using Chitosan/Poly (Acryl Amide-Acrylic Acid) Hydrogels: Characterization and Kinetic Study. *NeuroQuantology* 2021; 19(2): 31-37.

Jasim LS, Radhy ND, Jamel HO. Synthesis and Characterization of Poly (Acryl Amide-Maleic Acid) Hydrogel: Adsorption Kinetics of a Malachite Green from Aqueous Solutions. *Eurasian Journal of Analytical Chemistry* 2018; 13(1b): em74.

Chiban M, Carja G, Lehutu G, Sinan F. Equilibrium and thermodynamic studies for the removal of As (V) ions from aqueous solution using dried plants as adsorbents. *Arabian Journal of Chemistry* 2016; 9: S988-S999.

Zafar MN, Dar Q, Nawaz F, Zafar MN, Iqbal M, Nazar MF. Effective adsorptive removal of azo dyes over spherical ZnO nanoparticles. *Journal of Materials Research and Technology* 2019; 8(1): 713-725.

Radhy ND, Jasim LS. Synthesis of graphene oxide/hydrogel composites and their ability for efficient adsorption of crystal violet. *Journal of Pharmaceutical Sciences and Research* 2019; 11(2): 456-463.

Riegel M, Ellis PP. High-performance liquid chromatographic assay for antiinflammatory agents diclofenac and flurbiprofen in ocular fluids. *Journal of Chromatography B: Biomedical Sciences and Applications* 1994; 654(1): 140-145.

Raheem RA, Al-gubury HY, Aljeboree AM, Alkaim AF. Photocatalytic degradation of reactive green dye by using Zinc oxide. *Journal of Chemical and Pharmaceutical Science* 2016; 9(3): 1134-1138.

Shama SA. Spectrophotometric determination of phenylephrine HCl and orphenadrine citrate in pure and in dosage forms. *Journal of pharmaceutical and biomedical analysis* 2002; 30(4): 1385-1392.

Shen J, Cui C, Li J, Wang L. In situ synthesis of a silver-containing superabsorbent polymer via a greener method based on carboxymethyl celluloses. *Molecules* 2018; 23(10): 2483.

Speltini A, Merli D, Profumo A. Analytical application of carbon nanotubes, fullerenes and nanodiamonds in nanomaterials-based chromatographic stationary phases: A review. *Analytica chimica acta* 2013; 783: 1-16.

Abdulsahib WK, Ganduh SH, Radia ND, Jasim LS. New approach for sulfadiazine toxicity management using carboxymethyl cellulose grafted acrylamide hydrogel*. International Journal of Drug Delivery Technology* 2020; 10: 1-7.

Wang Z, Li S, Lv Q. Simultaneous determination of dihydroxybenzene isomers at single-wall carbon nanotube electrode. *Sensors and Actuators B: Chemical* 2007; 127(2): 420-425.

Ware GW. *Reviews of Environmental Contamination and Toxicology.* Springer, New York, 1992; 126: 100-115.

Zhao YD, Zhang WD, Chen H, Luo QM. Anodic oxidation of hydrazine at carbon nanotube powder microelectrode and its detection. *Talanta* 2002; 58(3): 529-534.

Li Y, Wang S, Zhang Y, Han R, Wei W. Enhanced tetracycline adsorption onto hydroxyapatite by Fe (III) incorporation. *Journal of Molecular Liquids* 2017; 247: 171-181.

Sodani M, Shahidi M, Zaker BS, Mehr RK. An investigation into the effectiveness of human givens and adlerian therapy on happiness and psychological well-being of students of shahid chamran university of ahvaz. *NeuroQuantology* 2019; 17(4): 18-25.